# Energy distribution near jet stream, and associated wave-amplitude relations

By CHESTER W. NEWTON and YUKIO OMOTO,[1] *National Center for Atmospheric Research, Boulder, Colorado*

(Manuscript received March 20; revised version June 21, 1965)

ABSTRACT

In a progressive wave system, the meander of the jet-stream axis typically exceeds the amplitude of the streamlines. This feature is shown to be required by both kinematic and energetic considerations. The specific energy (sum of stream function and kinetic energy) varies along the jet-stream axis, being greatest at the troughs and smallest at the ridges, in proportion to the celerity and amplitude of the wave pattern. In a synoptic example, it is demonstrated that the jet-stream axis is essentially advected by the wind in an isentropic surface, with satisfaction of energy requirements. Schematic illustrations are given, of some relationships between the jet-stream axis and the contour field.

## 1. Introduction

It is well-known that there is a tendency for the jet-stream axis to deviate across the isobaric contours when there are appreciable variations of wind speed along the current. In the most familiar instance, the jet axis crosses toward lower contours where the wind speed increases downstream, and vice versa. This is in accord with what is expected from energy considerations, a gain in kinetic energy of the air parcels taking place at the expense of a loss of potential energy (see MURRAY & DANIELS, 1953; RIEHL, 1954; RAETHJEN, 1958; NEWTON, 1959).

In many instances, however, this relationship is not so straightforward. Fig. 1 shows an example wherein it is apparently satisfied over southern Canada and the northern United States. Over the central and south-eastern States, on the other hand, the jet-stream axis is inclined toward *higher* contours despite a rather marked wind-speed *increase* in the downstream direction. Thus it is not apparent from a single map how energy relationships are satisfied for air particles near the jet stream A related feature is that the overall amplitude of the wave in the jet-stream axis is appreciably greater than the amplitude of the contours (by about 25 per cent, in this case). These aspects of wave structure will be shown to be essentially linked with progression of the wave pattern.

## 2. Distribution of specific energy

In the following discussion, an attempt will be made to demonstrate that air parcels do not cross the axis of the jet stream, or at any rate that such a crossing is not discernible during short periods of time.

In partial support of this proposition, one might consider the distribution of wind in Fig. 2, and of the isentropes in Fig. 3 (location of cross section shown in Fig. 5), these being fairly typical of the jet-stream region. On the left flank of the jet stream, the absolute vorticity is large and the stability is great, while on the right flank the opposite is true. Evidently the lateral movement of air parcels from the right flank to the left, or vice versa, would require a marked change of the potential vorticity.

[1] Present affiliation: Dept. of Geophysics, Faculty of Science, Hokkaido University, Sapporo, Hokkaido, Japan.

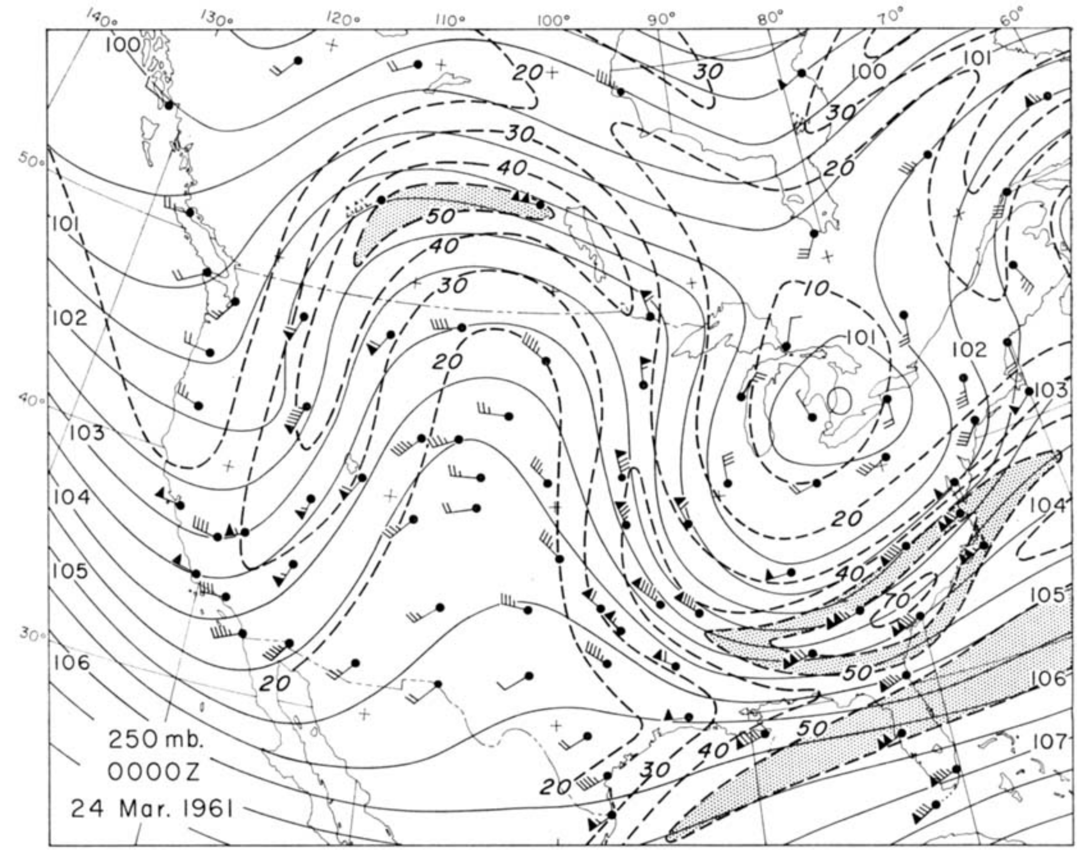


FIG. 1. 250-mb chart, 00 GCT 24 March 1961. Thin lines, geopotential contours (labelled in hundreds of meters); dashed lines, isotachs, labelled in m/sec (region with wind speed between 50 and 60 m/sec stippled). Wind symbols: flag, 50 kt; full barb, 10 kt (dashed where level of chart was not reached).

It is instructive also to look at the distribution of specific energy,[1]

$$E \equiv \psi + V^2/2, \tag{1}$$

where $\psi = (c_p T + gz)$ is the Montgomery potential or isentropic stream function. This is shown in Fig. 3 in the eastern trough, and in Fig. 4 in the ridge upstream.[2] The isopleths of $E$ are seen to be strongly packed in the neighborhood of the jet stream. Thus for an air particle to cross the jet stream laterally, a large change of specific energy would be required.

From both of the above considerations, the lateral movement of air across the jet stream, in the vicinity of the "tropopause break", appears not to be favored. It must be recognized, however, that these arguments apply to conditions in a given cross section, and that changes of potential vorticity or specific energy along the direction normal to the sections are not allowed for. It is perhaps more appropriate to inspect the distribution of $E$ at a particular isentropic surface. Fig. 5 shows this quantity, for the surface $\theta = 320°K$ which was on the average near the level of the polar-front jet stream.

If $n$ is a normal toward the right of a stream-

[1] Specific energy is defined, in the *Glossary of Meteorology* (HUSCHKE, 1959) according to usage in hydrology wherein only potential energy and kinetic energy of fluid motion are considered. In a compressible fluid the enthalpy and the latent heat energy must be included. Here the latter is omitted because its influence is negligible at high levels.

[2] In order to eliminate the overpowering variation of $E$ in the vertical, the quantity $(E - \bar{E})$ is portrayed, $\bar{E}$ being the mean value at a given isentropic surface, for all stations in each of the cross sections. The *lateral* gradient of $(E - \bar{E})$ along isentropic surfaces is the same as that of $E$.

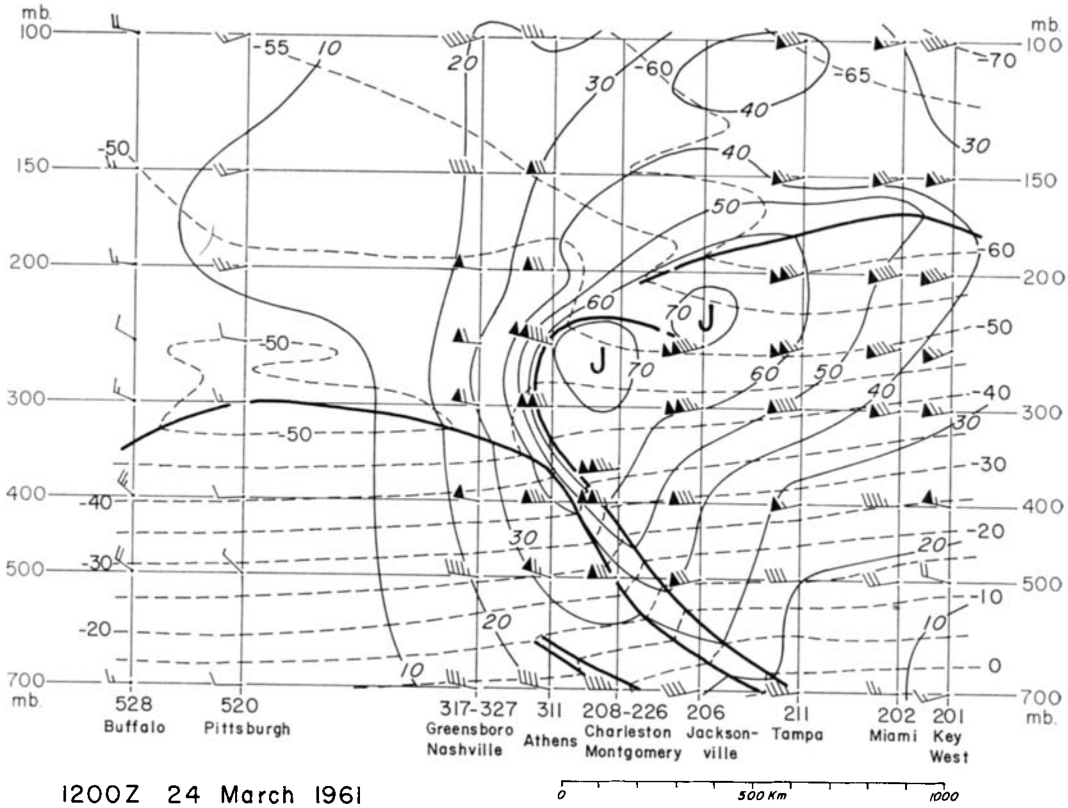


FIG. 2. Cross section along trough line in Fig. 5 (dotted line), showing isotherms (dashed, deg C) and isotachs (m/sec). Winds plotted with respect to north at top of figure.

line, and the wind speed greatly exceeds the speed of trough and ridge movement,

$$\left(\frac{\partial E}{\partial n}\right)_\theta \approx V\zeta_a, \tag{2}$$

where $\zeta_a = (K_s V + \partial V/\partial n + f)$ is the absolute vorticity in an isentropic surface. This follows from the operation $\partial/\partial n$ on Eq. (1), observing that $fV_g = \partial\psi/\partial n$, $KV^2 = f(V_g - V)$, and $K \approx K_s$, where $K$ is the curvature of a trajectory and $K_s$ that of a streamline.[1] Eq. (2) expresses the condition, apparent from the isopleths of Figs. 3 and 5, that the gradient of $E$ across the current is large near the jet stream and on its cyclonic flank, where both $V$ and $\zeta_a$ are large.

[1] Note that distant from the jet stream where $KV$ and $\partial V/\partial n$ diminish, $\zeta_a$ approaches $f$ and $E$ approaches $\psi$, so that Eq. (2) becomes approximately the geostrophic wind equation $\partial\psi/\partial n = fV_g$. Thus except near the jet stream, the fields of $E$ and $\psi$ are similar (cf. Fig. 8c).

Taking the derivative along the direction $s$ of the wind, and observing that in an isentropic surface

$$\frac{dV}{dt} = \frac{\partial V}{\partial t} + V\frac{\partial V}{\partial s}$$

and $dV/dt = -\partial\psi/\partial s$,

we find that
$$\frac{\partial E}{\partial s} = -\frac{\partial V}{\partial t}. \tag{3}$$

Let Fig. 6 be a portion of the jet stream, west of a trough which progresses eastward without change in configuration of the velocity field. The wind speed then increases locally with time on the cyclonic flank of the jet stream, and decreases with time on its anticyclonic flank. The isopleths of $E$ are arranged in the only form compatible with Eqs. (2) and (3). Eq. (2) states that if there is a discontinuity of vorticity (in the form of an abrupt change of shear)

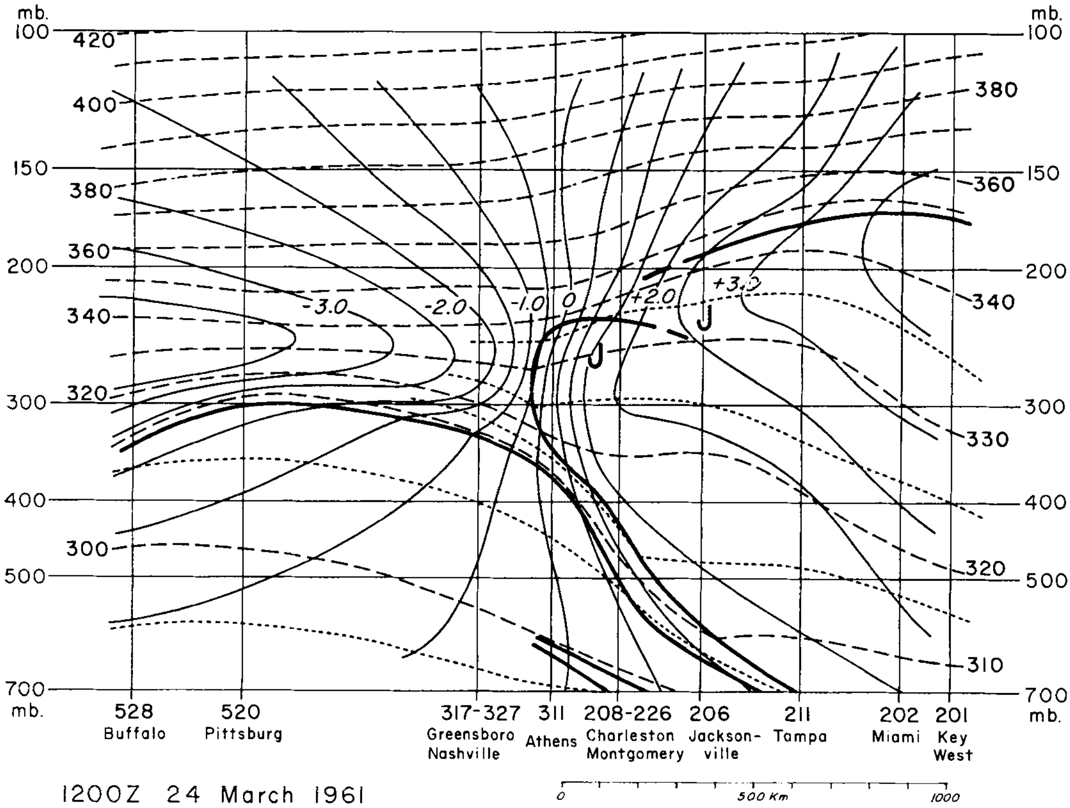


FIG. 3. For section of Fig. 2, the distribution of potential temperature (dashed lines, deg K) and relative distribution of specific energy (solid lines; see text). Units of latter are $10^3$ m$^2$/sec$^2$.

across the jet, there must be a discontinuity of $\partial E/\partial n$. In order to satisfy Eq. (3), the wind must blow toward higher values of $E$ on the anticyclonic flank and toward lower values of $E$ on the cyclonic flank, in this portion of the wave pattern, as indicated by the streamline in the sketch. This shows that *in a progressive jet stream wave, the streamlines must cross toward the cyclonic-shear side of the jet axis upstream from a trough, and toward the anticyclonic-shear side downstream from a trough.*[1] It is evident that in a *stationary* system, the specific-energy isopleths as well as the streamlines are parallel to the jet stream.

[1] More generally, a local change of wind speed may take place partly as a result of movements of isotach maxima and minima along the direction of the jet stream. Immediately next to the jet-stream core, the contribution from this influence on $\partial V/\partial t$ and $\partial E/\partial s$ is the same on the cyclonic- and anticyclonic-shear sides. It can be shown that the italicized statement is valid regardless of the configuration or progression of the velocity field.

Eq. (3) is simply a statement, in another form, of the energy equation developed by V. BJERKNES (1917; see also HAURWITZ, 1941),

$$\frac{dE}{dt} = \frac{\partial \varphi}{\partial t}. \tag{4}$$

This is valid for adiabatic frictionless motion.

## 3. Jet stream-streamline amplitude relationship

The preceding considerations suggest that, *near the level of maximum wind, the jet-stream axis should be essentially a material curve which moves with the velocity of the horizontal wind.* SAWYER (1950) cited observations which indicated, in agreement with this proposition, that the jet axis moves approximately with the component of wind normal to it.

Fig. 7 shows schematically two successive

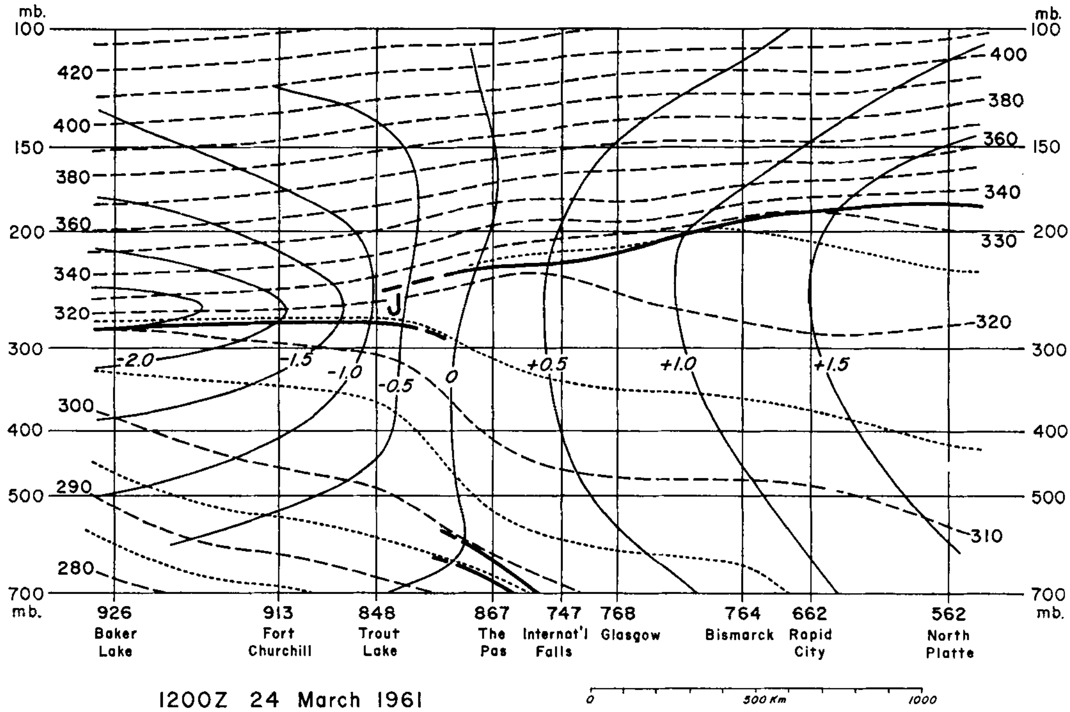


FIG. 4. Same as Fig. 3, section in ridge, along dotted line in Fig. 5.

positions of a streamline and of the jet-stream axis. If the streamline wave system is progressive, the jet-stream wave can only progress with it if there is a non-parallelism of the two systems of lines in the manner shown. This is compatible with the discussion of Fig. 6 above. It is clear from Fig. 7 that *if the jet-stream axis is displaced with the air trajectories, it must have an amplitude greater than that of the streamline system,* as in Fig. 1.

According to the postulated condition that air particles remain in the jet axis, a particle originating on a crest of the jet-stream wave would follow a trajectory to the downstream trough of the jetstream wave at some later time. The amplitude of the air-particle trajectory would thus also be the amplitude $A_J$ of the jet-stream wave (Fig. 7). If $V$ is the wind speed in the jet axis, $C$ the phase speed and $A_S$ the streamline amplitude of the wave, we may then write

$$\frac{A_J}{A_S} = \frac{V}{V-C}, \tag{5}$$

by analogy with the familiar expression for the trajectory-streamline amplitude ratio employed by ROSSBY (1942) and by BJERKNES & HOLMBOE (1944) in a different but related context.

If air particles move along the jet-stream axis at constant speed (the speed in the jet core being the same at trough and ridge), then in the neighborhood of the jet axis the streamlines are parallel to contours of an isobaric surface. In that case, it may be inferred that the jet-stream axis meanders about the contours in the same manner as it meanders about a streamline.[1]

This conclusion is also reached if one considers the energetic requirement stated by Eq. (4), which may be written

$$\frac{d}{dt}\left(\frac{V^2}{2} + \psi\right) = \frac{\partial \psi}{\partial t}. \tag{4a}$$

[1] This is more properly said of the streamfunction isopleths in an isentropic surface; however near the level of maximum wind the same is true of the isobaric contours. In the middle troposphere where there is appreciable vertical shear and vertical motion, the streamlines may deviate appreciably from the isobaric contours (see, for example, the discussion by NEWTON & PALMÉN, 1963).

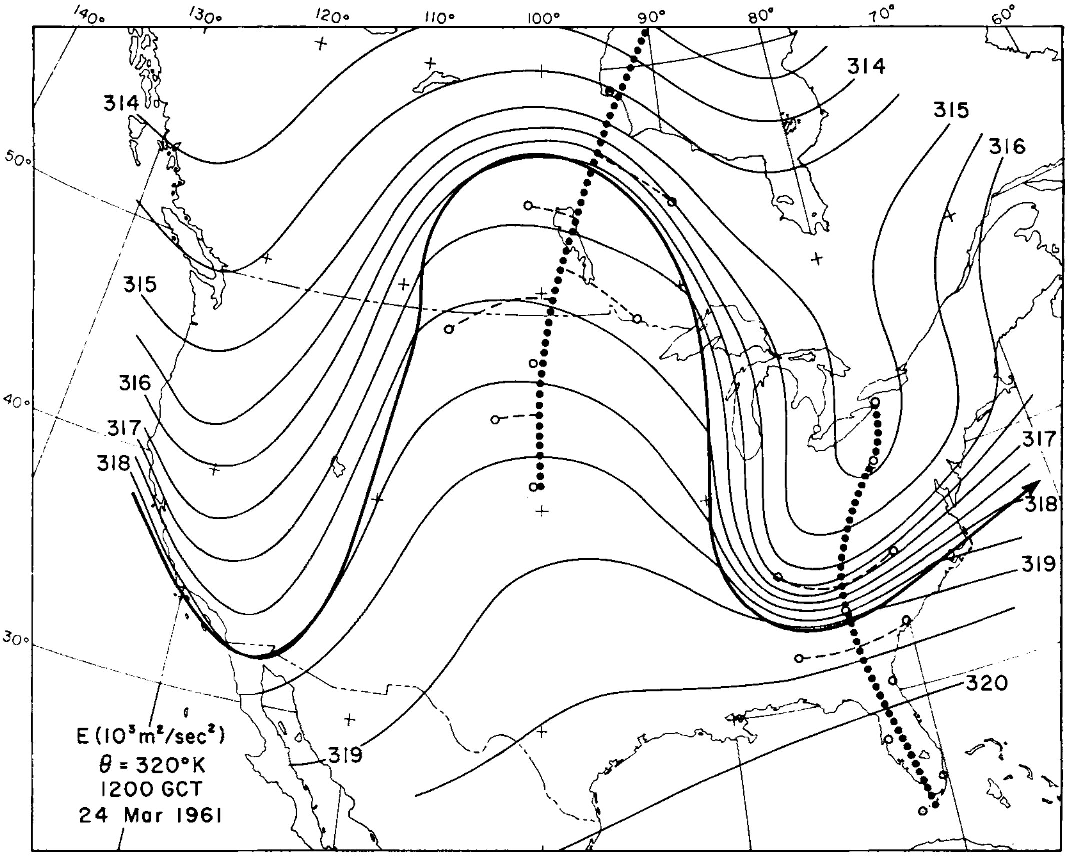


FIG. 5. Specific energy (units $10^3$ m²/sec²) at 320°K isentropic surface, 12 GCT 24 March 1961. Heavy line is jet-stream axis.

From inspection of the central trajectory in Fig. 7, it is seen that a particle undergoing no speed acceleration between times $t_0$ and $t_0 + \delta t$ would undergo an individual increase of potential,[1] consistent with Eq. (4a), by virtue of movement of the system which results in a local increase of $\psi$ in this region.

Integrating over the time $\tau$ required for an air parcel in the jet axis to travel from ridge $R$ to trough $T$ (see discussion by DANIELSEN, 1961),

$$\left(\frac{V^2}{2} + \psi\right)_T - \left(\frac{V^2}{2} + \psi\right)_R = \overline{\frac{\partial \psi}{\partial t}}\tau. \qquad (6)$$

Here the bar signifies a time-average over the path followed by the particle. Eq. (6) shows that *in a progressive wave system with no change of wind speed along the jet axis, the jet axis must meander between lower potential in ridges and higher potential in troughs.* Since about 24 to 36 hrs are required for an air particle in the jet axis to pass from ridge to trough or trough to ridge in a large-amplitude long-wave system, and the local potential change may amount to several hundreds of meters in this time, the cross-contour deviation of the jet axis between ridge and trough is similarly large. The corresponding geometrical deviation may be several hundreds of kilometers.

## 4. Trajectories and movement of jet axis

Three isentropic charts at the surface 320°K, at 12-hr intervals, are shown in Fig. 8. These

[1] Hereafter for convenience, "potential" will denote either the isentropic stream function or the isobaric geopotential, depending on the context. The unit $10^3$ m²/sec² or $10^7$ erg/gm for $E$ or $\psi$ corresponds closely to 100 m dynamic height.

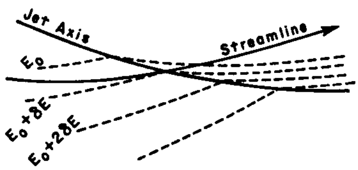


FIG. 6. Schematic distribution of specific energy. See text.

illustrate the varying amounts of data available, particularly with regard to wind information, and give some impression of the uncertainties in analyzing the wind and stream function fields. For example, it is clearly possible to establish that the jet stream has a much larger amplitude than the streamlines, but at the same time the jet axis could be mislocated by 100 km in some regions such as

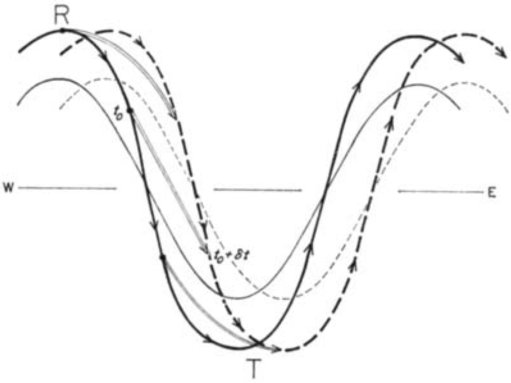


FIG. 7. Showing relation of a streamline (thin line) to the jet stream axis (heavy line). Solid curves correspond to an initial time $t_0$, and dashed lines to a time $\delta t$ later. Arrows on left side are particle trajectories.

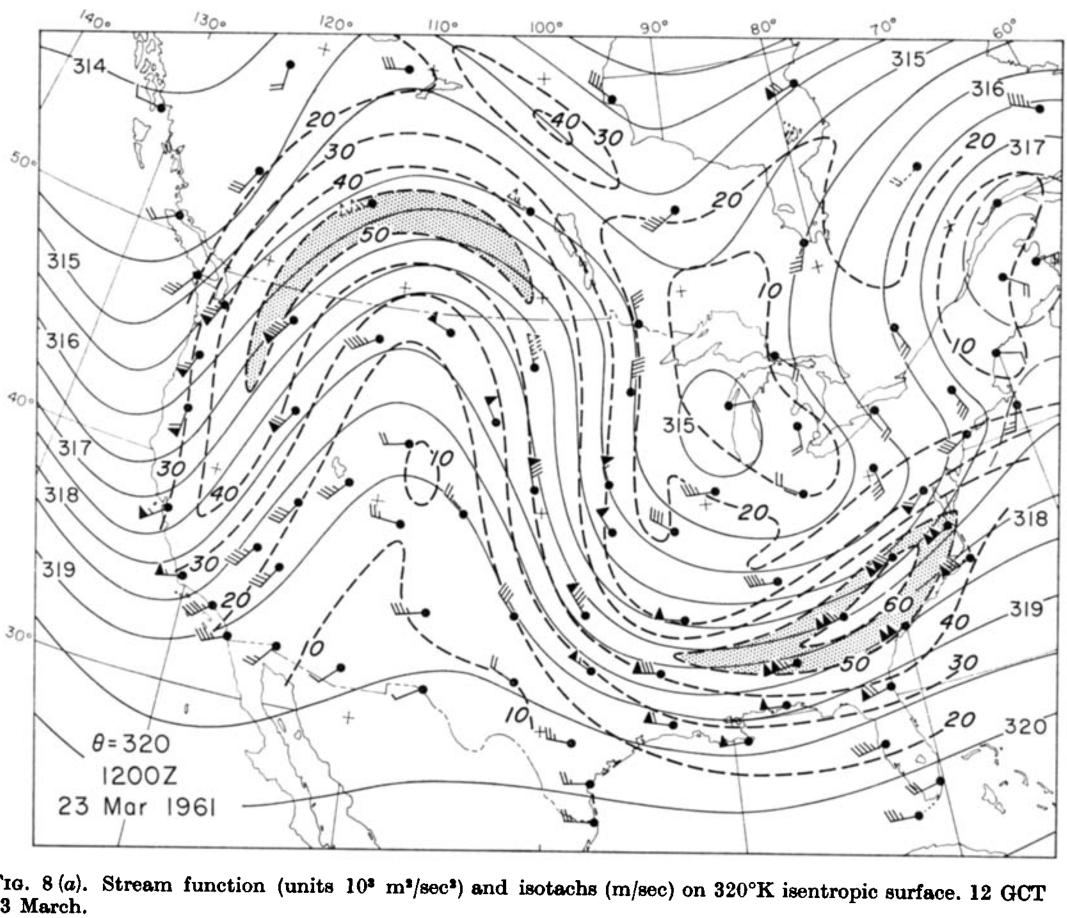


FIG. 8 (a). Stream function (units $10^3$ $m^2/sec^2$) and isotachs (m/sec) on 320°K isentropic surface. 12 GCT 23 March.

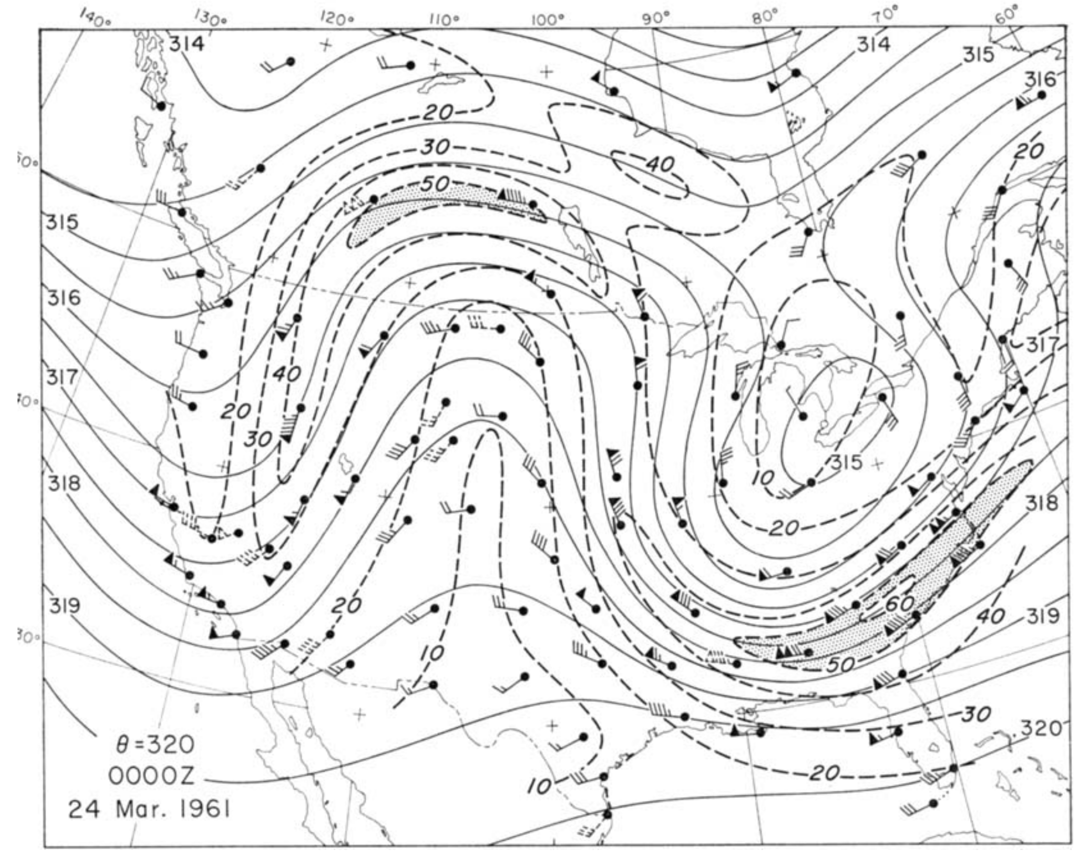


FIG. 8 (*b*). Stream function (units $10^3\,m^2/sec^2$) and isotachs (m/sec) on 320°K isentropic surface. 00 GCT 24 March.

southern Canada.[1] It may also be noted that the configuration of the polar-front jet stream is very similar to that on the isobaric chart of Fig. 1 (although the isentropic surface lies below the level of the subtropical jet seen on the isobaric chart).

The locations of the jet axis, taken from Figs. 8*b* and 8*c*, are shown at 00 GCT and 12 GCT 24 March in Fig. 9*a*, along with 12-hr trajectories starting on the jet axis at the earlier time. These trajectories were constructed from isogon and isotach charts. Winds were interpolated each 3 hr between charts, the directions being laid out with a protractor and the length of each 3-hr segment being consistent with the wind speeds at its beginning and end.

Although the terminal points of some trajectories are satisfyingly close to the jet axis at the second time, others either overshot or undershot the jet location. This is believed to be due to random errors. Such trajectories were constructed for the five 12-hr periods between 00 GCT 23 March and 12 GCT 25 March. The deviations of the terminal points toward the right or left side of the jet axis were approximately normally distributed, with a root-mean-square deviation of 0.96 deg lat from the arithmetic mean of zero. Considering that the average length of a 12-hr trajectory is about 15 to 20 deg lat, this size of error in location would correspond to an average error in direction of the trajectory of about 3°. This probably does not exceed the accuracy with which the isogon

[1] In locating the jet axis, use was made of continuity and also of cross sections such as Fig. 4, which shows that the baroclinity was greatest between Trout Lake and The Pas so that the general location of the jet axis is correct in Fig. 8*c*.

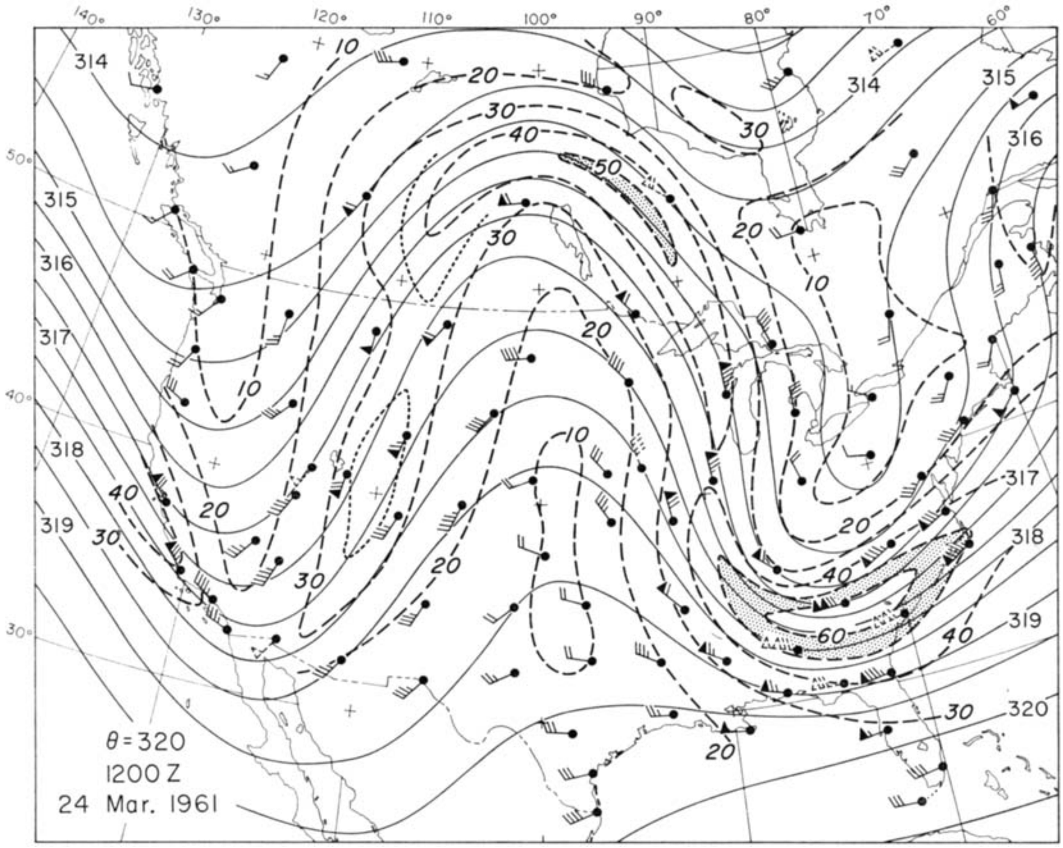


Fig. 8 (c). Stream function (units $10^3\ m^2/sec^2$) and isotachs (m/sec) on 320°K isentropic surface. 12 GCT 24 March.

field can be analyzed. Contributions to the error can also result from uncertainties in wind speed, and uncertainties in location of the jet axis both at the beginning and end of the trajectories. Thus it appears justifiable to infer that, over short periods of time, an air particle initially in the jet-stream axis remains in it.

Accordingly, as a next step the trajectories such as those in Fig. 9*a* were adjusted so that their terminal points lay on the jet axis. The adjusted trajectories were then tested against Eq. (6), applying this formula over lengths of the 12-hr trajectories,

$$\Delta E = \overline{\frac{\partial \psi}{\partial t}} \cdot 12 \text{ hr}, \tag{7}$$

where $\Delta E$ is the specific-energy change between beginning and end of the trajectory. The 12-hr potential change over the period covered by Fig. 9*a* is shown in Fig. 9*b*, illustrating that the southwesterly trajectories were in regions of decreasing $\psi$, and the northwesterly trajectories in regions of increasing $\psi$. From computations based on the $\psi$ gradients and the speed of progression of the pattern, it was verified that the 12-hr changes provide a close estimate of the instantaneous tendencies in this case.

The tendency $\delta\psi/\delta t$ was interpolated between successive charts, for 3-hr segments of each trajectory, and the resulting values were summed to obtain the right side of Eq. (7). Values of $V$ and $\psi$ were then read off at the beginning- and end-points of each trajectory, and the quantity on the left of Eq. (7) computed.

The resulting values for the left and right sides of Eq. (7) are plotted respectively as ordinate and abscissa in Fig. 10. It must be recognized that even though the trajectory end-points were adjusted to lie on the jet axis,

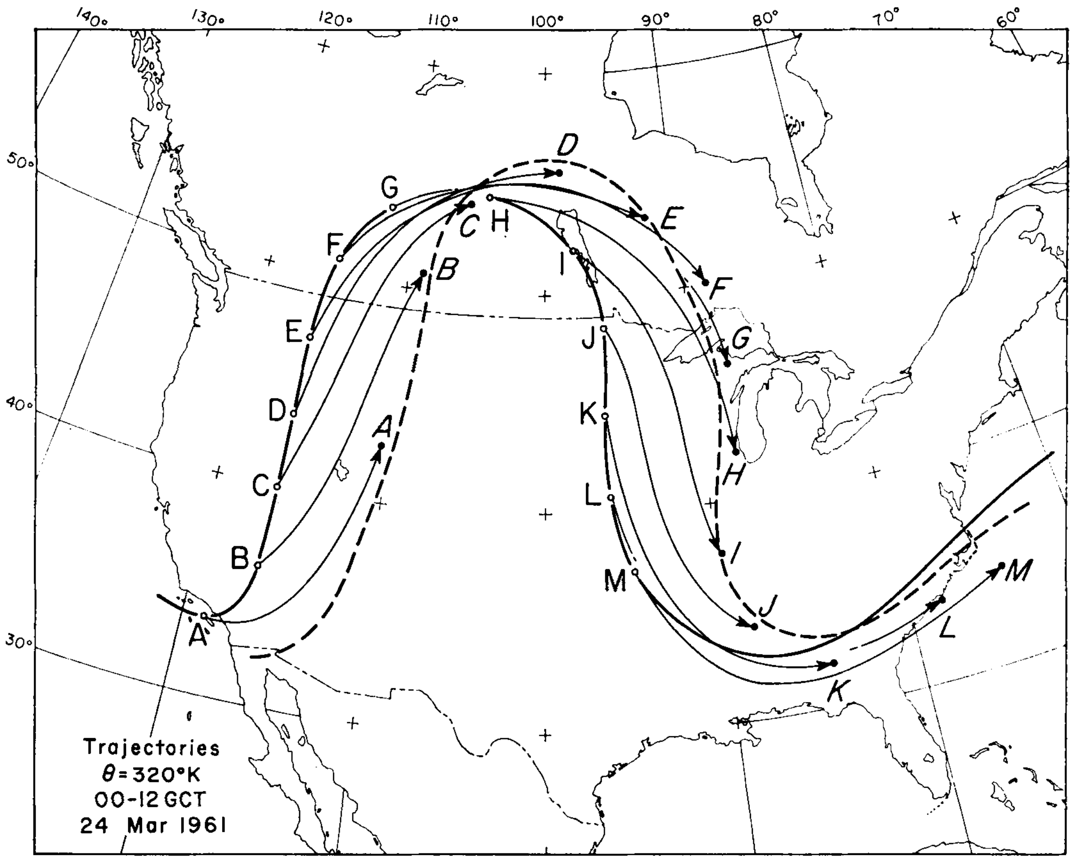


FIG. 9. (*a*) Locations of jet axes on 320°K isentropic surface, at 00 GCT (heavy solid line) and 12 GCT 24 March (dashed). Thin lines show 12-hr trajectories based on wind analyses.

inexact location of the jet axis itself can contribute to errors in the evaluation of $\Delta E$. For example, in the map of Fig. 8*c*, an error of only 0.5 deg lat in placing the jet axis would result in an error in evaluating $\psi$, of 200 to 400 m$^2$/sec$^2$, depending on the place in the wave system. Also, errors of perhaps 200 to 300 m$^2$/sec$^2$ may be present in the analysis of $\psi$, due to inaccuracies of observations (a mean temperature error of 0.5°C, between the ground and the 300-mb level, would result in an error of 200 m$^2$/sec$^2$). The wind speed in the jet core is also considered to be uncertain, in places, by as much as 3 to 5 m/sec, and this could result in an error up to 300 m$^2$/sec$^2$ in $V^2/2$.

Considering the possible errors noted above, the scatter in Fig. 10 is thought to be largely due to uncertainties in observations and analysis. Allowing for this, it may be concluded that since the points cluster about the 1:1 line, *the energy relationship is satisfied for particles on the assumption that they remain in the jet axis.*

Trajectories constructed for other cases (for example, the case described from other viewpoints by NEWTON & PALMÉN, 1963), utilizing isobaric analyses near the level of maximum wind, further indicated that the jet-stream core is advected with the air trajectories. The jet axis-contour relationship implied by Eq. (6) is usually evident in moving wave patterns, whenever there are enough observations to establish the velocity field reliably.

## 5. Conclusion

It has been shown that near the level of maximum wind, the axis of the jet stream must exhibit a systematic meandering across the streamlines, in order to satisfy energetic as well as kinematic requirements in a moving

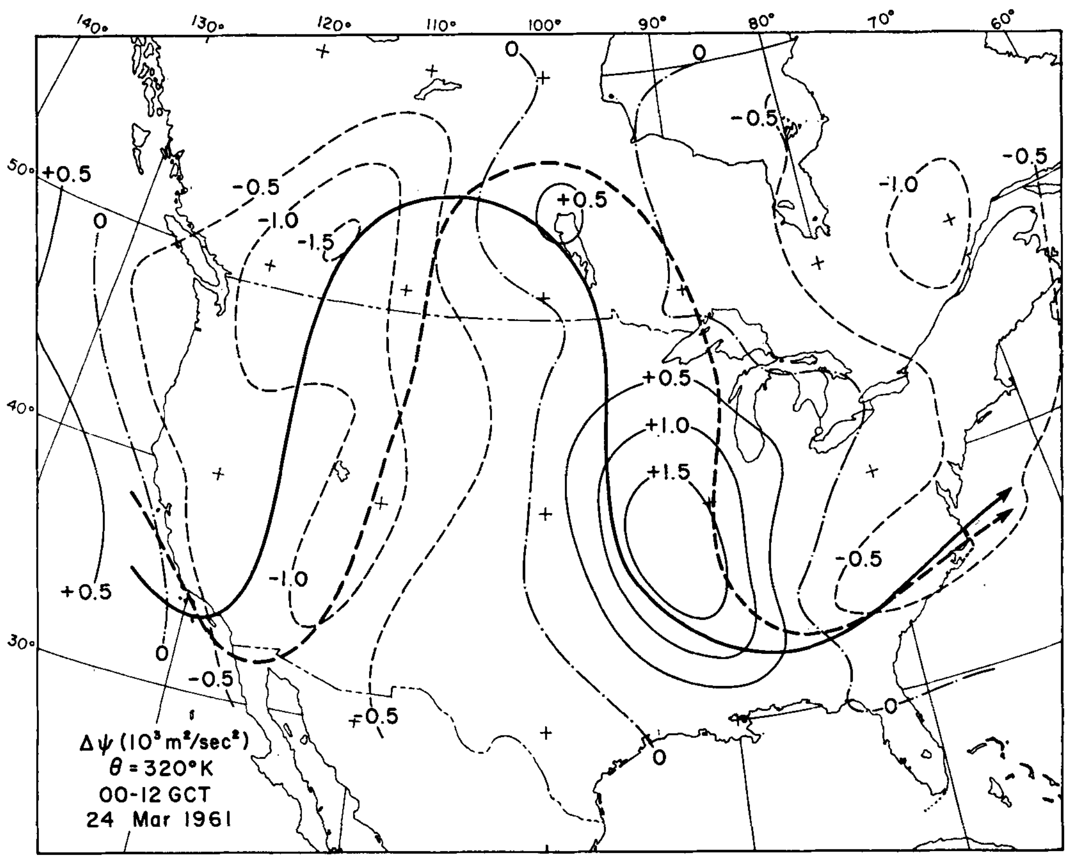


FIG. 9 (b) 12-hr change of stream function (units $10^3$ m²/sec²).

wave system. This meandering is different in nature from, and may augment or diminish, the cross-contour meandering normally associated with wind-speed variations along the jet axis. The synoptic cases support the notion that although there may be a slow drift of air across the jet axis, that axis near the level of maximum wind is essentially advected with the wind, when short time periods are considered.

Fig. 11 summarizes, in schematic fashion, some possible configurations of the jet-stream axis relative to the contour pattern. In Fig. 11 *a*, a stationary wave with no speed variation along the jet axis, the jet would be parallel to the contours. In a progressive wave pattern (Fig. 11 *b*), the jet axis meanders with a greater amplitude than the contours. Height rises to the west of and falls to the east of the troughs go hand-in-hand with a deviation of the jet axis toward higher geopotential west of the trough and toward lower geopotential on its east side, in accordance with Eq. (6).

Referring to Fig. 7, the jet-stream wave can only move if there is a component of wind normal to the jet axis; from Fig. 11 *b* this component (with the geostrophic approximation) would be measured by the potential gradient along the jet axis. The *eastward* component of this wind advecting the jet-stream axis would in turn be given (for the case of Fig. 11 *b*) by

$$\frac{1}{\bar{f}}\frac{(\psi_T-\psi_R)}{2A_J}\approx C.$$

Thus $(\psi_T-\psi_R)\approx 2\bar{f}CA_J$, showing that the difference in potential between jet-axis trough and ridge is greatest when the wave amplitude itself is large and the wave system is fast-moving. The same conclusion could be arrived at from Eqs. (5) or (6), which are based on

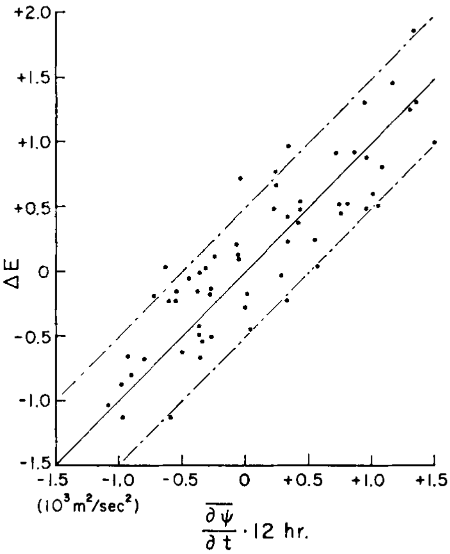


Fig. 10. Change of specific energy, *vs.* integrated local change of $\psi$ following air parcels. Each point represents a trajectory such as in Fig. 9*a*. Dash-dotted lines correspond to discrepancies of $\pm 500$ m²/sec².

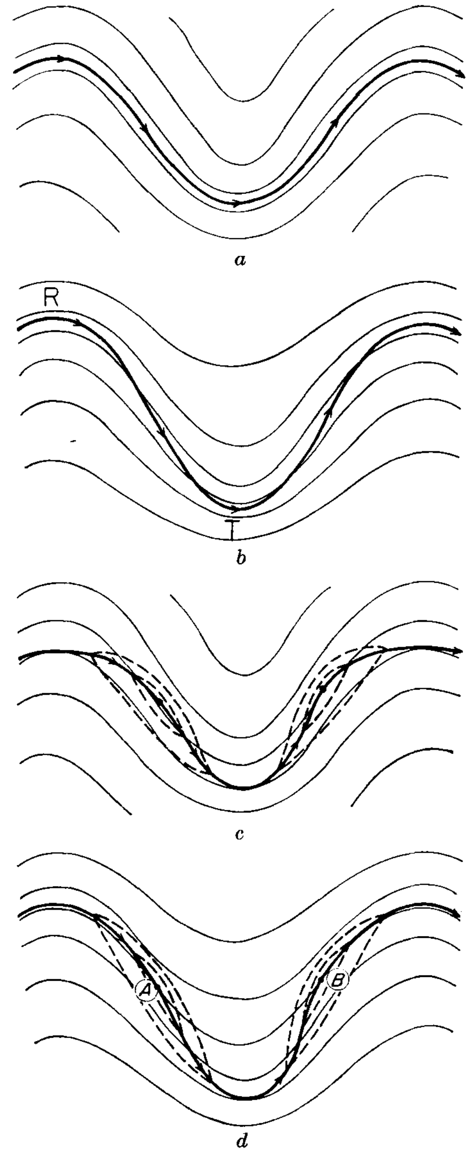


Fig. 11. Schematic relations between jet-stream axis and contours. In (*c*) and (*d*), dashed lines are isotachs. $a$ = Stationary wave, $V$ constant along jet axis; $b$ = Progressive wave, $V$ constant along jet axis; $c$ = Stationary wave, $V$ variable along jet axis; $d$ = Progressive wave, $V$ variable along jet axis.

independent considerations and are shown in the Appendix to be mutually compatible.

The patterns in Figs. 11*c* and 11*d* correspond to the same systems, when a wind-speed maximum is superimposed near the inflections of the wave pattern. In Fig. 11*d*, the cross-contour deviation due to wind-speed variations along the current is accentuated downstream from *A* and upstream from *B*. Upstream from *A* and downstream from *B* the deviation due to this influence is diminished (compare Fig. 11*b*), in accord with Eq. (6). The most extreme meandering of the jet axis relative to the contours is naturally to be expected when the strongest winds are located in the wave crests, and the least when the strongest wind is in the troughs.

Knowledge of the probable relationships between jet-stream and contour amplitudes, as developed above, can be of assistance in analyzing the wind field where, as frequently happens, this is adequately defined by the observations in part but not all of the wave system. These relationships are compatible with the considerations discussed by Bjerknes (1951) and the illustrations by Palmén (1951), which indicate that the polar-front zone is farther poleward in ridges and farther equatorward in troughs, than a given contour describing the upper-tropospheric flow pattern.

Since for practical reasons only short time periods can be dealt with, and even the most exacting analysis cannot resolve the velocity field with an accuracy greater than 1 to 3 m/sec, the above analysis does not preclude the possibility of a slow drift of air across the jet-stream axis. Such a drift is, for example, indicated by the northward upper branch of the Hadley cell, which extends north of the mean latitude of the subtropical jet stream in winter (KRISHNAMURTI, 1961). It is also suggested by the circulation in experiments with a rotating dishpan (RIEHL & FULTZ, 1957). However, the mechanism by which the drift takes place has not been investigated in detail. It is possible that it occurs, for example, in places where the jet stream is not continuous around the hemisphere but where the segments of strongest wind have an overlapping structure.

In any event, the high correlation between potential vorticity and radioactivity concentration, found by DANIELSEN, BERGMAN & PAULSON (1962), suggests a reluctance for material to find its way from the polar stratosphere to the troposphere through the "tropopause break" at jet-stream level. The analyses by STALEY (1960) and REITER (1963) demonstrate how radioactive material may be transferred across the jet stream, by becoming incorporated into a frontal layer or the upper troposphere of the cold air, and descending in trajectories crossing beneath the jet-stream axis at a lower level. PALMÉN (1951) was the first to point out clearly that trajectories in subsiding air masses differ greatly from horizontal trajectories, making possible an exchange in this manner.

APPENDIX

## Compatibility of kinematic and energetic requirements

Eq. (5) is strictly applicable to a wave system of small amplitude which moves without change of shape, and in which the wind speed is uniform along the current. With the latter condition, Eq. (6) reduces simply to

$$\psi_T - \psi_R = \overline{\frac{\partial \psi}{\partial t}}\,\tau. \tag{8}$$

Referring to Fig. 7 where the thin lines may now be taken as an isopotential, we may write

$$\psi_T - \psi_R \approx 2(A_J - A_S)\frac{\partial \psi}{\partial y},$$

where $\partial\psi/\partial y$ is the $\psi$ gradient in ridge or trough, between the isopotential whose amplitude is $A_S$ and the jet axis whose amplitude is $A_J$. Employing the geostrophic approximation,

$$\psi_T - \psi_R \approx -2fV(A_J - A_S). \tag{9}$$

For a wave moving with speed $C$,

$$\overline{\frac{\partial \psi}{\partial t}} = -C\overline{\frac{\partial \psi}{\partial x}}, \tag{10}$$

where the bars correspond to space averages between ridge and trough. In a small-amplitude system with constant wind speed along the current, $\overline{\partial\psi/\partial t}$ is also the time-averaged $\psi$ tendency for a particle moving between ridge and trough, consistent with the meaning in Eq. (6). With the geostrophic approximation, if $\bar{v}$ is the mean south-north component of wind between ridge and trough, Eq. (10) may be written

$$\overline{\frac{\partial \psi}{\partial t}} = -Cf\bar{v}. \tag{11}$$

Since $\tau$ is the time required for an air particle to go from ridge to trough, $\bar{v}\tau = 2A_J$. On insertion into Eq. (11),

$$\overline{\frac{\partial \psi}{\partial t}}\,\tau = -2CfA_J. \tag{12}$$

Substitution for the terms of Eq. (8) from Eqs. (9) and (12) gives Eq. (5). Thus for a wave system of small amplitude, *the expressions based on kinematic and energetic requirements are compatible.* For large amplitudes, the above treatment is not strictly valid, partly because the geostrophic approximation has been used. However, it may be noted that the potential gradient would be overestimated by the geostrophic assumption in ridges, and underestimated in troughs; these two influences would tend to compensate each other in deriving Eq. (9) from the previous expression.

## Acknowledgements

We are indebted to Dr. Paul Julian and Mrs. Jean Smith for making available computations of stream functions and specific energies, based partly on a program by K. Bergman and D. Houghton. We also thank Mr. Ralph Coleman who drafted the figures, and Mr. Dennis Tussey who assisted with the computations.

## REFERENCES


BJERKNES, J., 1951, Extratropical cyclones. In: *Compendium of Meteorology* (T. F. Malone, Ed.), Boston, Amer. Meteor. Soc., pp. 577–598.

BJERKNES, J., and HOLMBOE, J., 1944, On the theory of cyclones. *J. Meteor.*, **1**, pp. 1–22.

BJERKNES, V., 1917, Theoretisch-meteorologische Mitteilungen. 4. Die hydrodynamisch-thermodynamische Energiegleichung. *Meteor. Z.*, **34**, pp. 166–176.

DANIELSEN, E. F., 1961, Trajectories: Isobaric, isentropic and actual. *J. Meteor.*, **18**, pp. 479–486.

DANIELSEN, E. F., BERGMAN, K. H., and PAULSON, C. A., 1962, *Radioisotopes, potential temperature and potential vorticity. A study of stratospheric-tropospheric exchange processes.* Dept. Meteor. and Clim., Univ. of Washington, 54 pp.

HAURWITZ, B., 1941, *Dynamic Meteorology.* New York, McGraw-Hill, 365 pp. (see pp. 238–240).

HUSCHKE, R. E. (Ed.) 1959, *Glossary of Meteorology.* Boston, Amer. Meteor. Soc., 638 pp. (see p. 529).

KRISHNAMURTI, T. N., 1961, The subtropical jet stream of winter. *J. Meteor.*, **18**, pp. 172–191.

MURRAY, R., and DANIELS, S. M., 1953, Transverse flow at entrance and exit to jet streams. *Quart. J. Roy. Meteor. Soc.*, **79**, pp. 236–241.

NEWTON, C. W., 1959, Axial velocity streaks in the jet stream: Ageostrophic "inertial" oscillations. *J. Meteor.*, **16**, pp. 638–645.

NEWTON, C. W., and PALMÉN, E., 1963, Kinematic and thermal properties of a large-amplitude wave in the westerlies. *Tellus*, **15**, pp. 99–119.

PALMÉN, E., 1951, The aerology of extratropical disturbances. In: *Compendium of Meteorology* (T. F. Malone, Ed.), Boston, Amer. Meteor. Soc., pp. 599–620.

RAETHJEN, P., 1958, Trägheitsellipse und jet stream. *Geophysica* (Helsinki), **6**, pp. 439–453.

REITER, E. R., 1963, A case study of radioactive fallout. *J. Appl. Meteor.*, **2**, pp. 691–705.

RIEHL, H., 1954, Jet stream flight, 23 March 1953. *Archiv. Meteor., Geoph., Bioklim., Ser. A*, **7**, pp. 56–66. (Discussion reproduced in Riehl, 1962, *Jet streams of the atmosphere.* Tech. Rep. No. 32, Dept. of Atmos. Sci., Colo. State Univ., Ft. Collins, Colo.)

RIEHL, H., and FULTZ, D., 1957, Jet stream and long waves in a steady rotating-dishpan experiment: structure of the circulation. *Quart. J. Roy. Meteor. Soc.*, **83**, pp. 215–231.

ROSSBY, C.-G., 1942, Kinematic and hydrostatic properties of certain long waves in the westerlies. *Univ. Chicago, Dept. Meteor., Misc. Reps.*, No. 5, 37 pp.

SAWYER, J. S., 1950, The movement of jet streams and the wind hodograph. *Meteor. Mag.*, **79**, pp. 357–358.

STALEY, D. O., 1960, Evaluation of potential vorticity changes near the tropopause and the related vertical motions, vertical advection of vorticity, and transfer of radioactive debris from stratosphere to troposphere. *J. Meteor.*, **17**, pp. 591–620.